New EAM potential for the Ni-Al system
and
Application to the martensitic transformation in B2-NiAl

G. P. Pun and Y. Mishin

Department of Physics
George Mason University

Supported by NASA

Development a new Ni-Al potential

Motivation

Some of the existing potentials for the Ni-Al system:

- **Voter and Chen** (MRS Proc., 1987)
- **Foiles and Daw** (JRM, 1987)
- **"B2-potential"** (Phys. Rev. B, 2002)
  - Strengths: Accurate fit to phase stability, point defect, GSF's and many other properties of B2-NiAl.
  - Weaknesses: less accurate for $L1_2$-Ni_3Al. Poor quality of the pure Ni and Al potentials
- **"Ni_3Al-potential"** (Acta Mater., 2004)
  - Strengths: excellent fit to Ni_3Al properties. Reproduces phase stability and the Ni-Al phase diagram.
  - Weaknesses: Less accurate for B2-NiAl. The pure Ni and Al potentials are accurate but Al is different from the widely used "Al-99"

Goals of the potential development

- Cross-fit our most favorite potentials “Al-99” and “Ni-04”
- Make it applicable to NiAl particles in Al matrix
- Further improve phase stability, with nearly accurate fits for both the B2 and $L1_2$ phases
- Check is the new potential will automatically reproduce the B2-$L1_0$ martensitic transformation

Approach:

- Use a larger database (experimental and *ab initio*) and improved fitting/testing methodologies
- Extensive testing for properties, especially the martensitic transformation

Fitting and testing procedures

Database

- Experimental properties:

  Lattice parameter, cohesive energy and elastic constants of B2-NiAl

- Ab initio data:

  Formation energies of several stable or unstable intermetallic compounds across the entire composition range

Optimization

- Minimization of mean-squared deviation from target properties. The weights control the priority of properties
- Simulated annealing by the simplex method

Potential functions

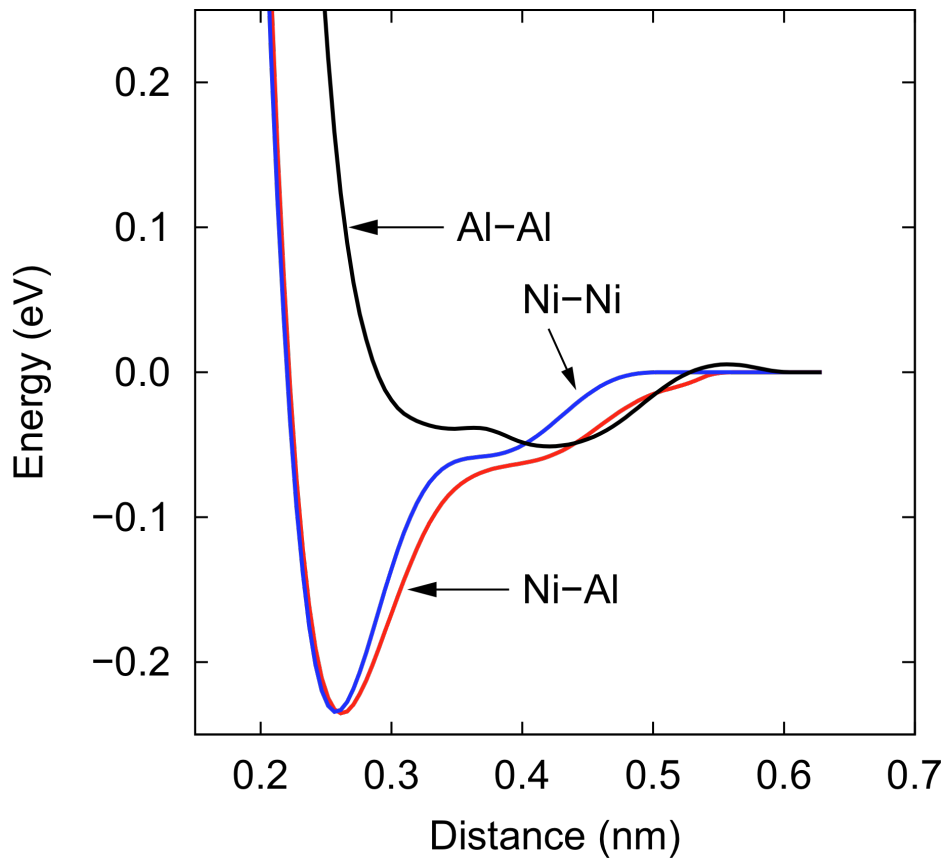

Pair-interaction functions of the Ni-Al potentials shown in the effective pair format.

Properties of B2-NiAl

Lattice properties

	Experiment	EAM (present)	"B2-NiAl"
a_0 (Å)	2.88	2.8320	2.86
E_f (eV)	-0.70	-0.6059	-0.56
E_0 (eV/atom)	-4.50	-4.5109	-4.47
c_{11} (GPa)	199	191	200
c_{12} (GPa)	137	143	140
c_{44} (GPa)	116	121	120

Surfaces and interfaces

	Experiment	*Ab initio*	EAM (present)	"B2-NiAl"
Surface				
(100)		2.85, 2.75	2.12	1.67
(110)		2.05, 1.87, 1.79, 1.37	1.89	1.25
(111)			2.20	1.63
APB				
(110)	>0.50	0.88, 0.81	0.65	0.55
(211)	>0.75	0.89, 0.99	0.73	0.72

Generalized stacking faults in B2-NiAl

Gamma-surfaces

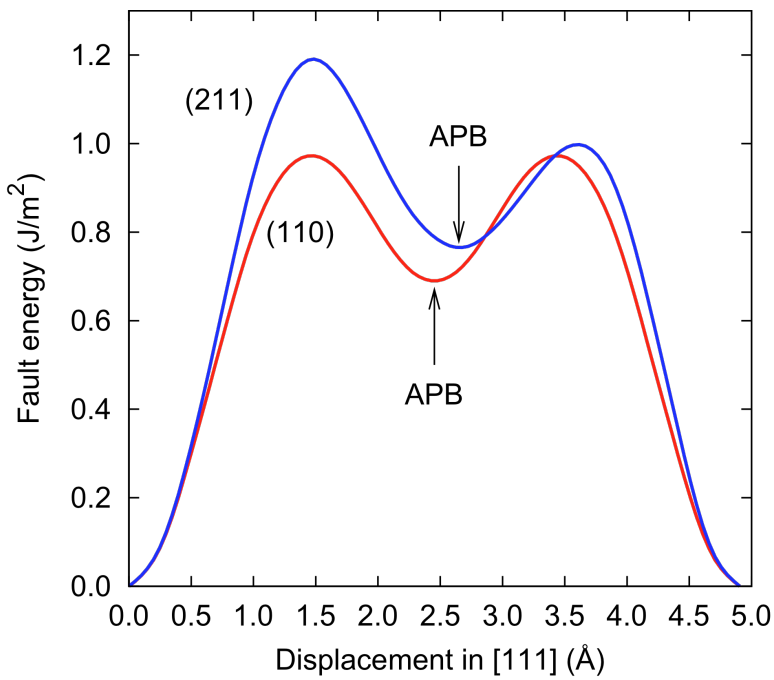

<111>{011} slip

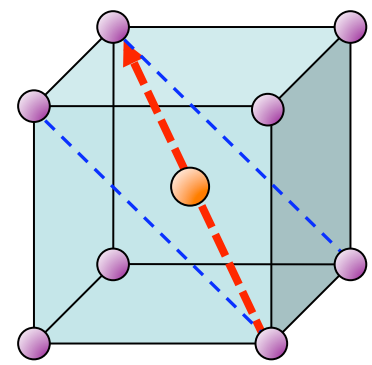

<111>{211} slip

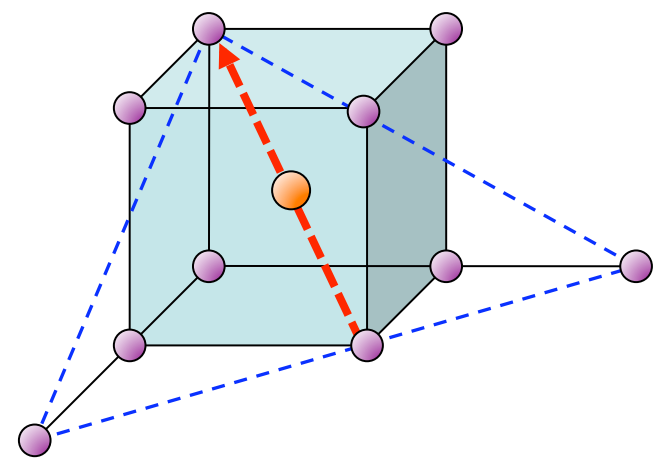

Ni Al

Phonon frequencies in B2-NiAl

Dispersion relations

Points – experiment
Lines – new potential

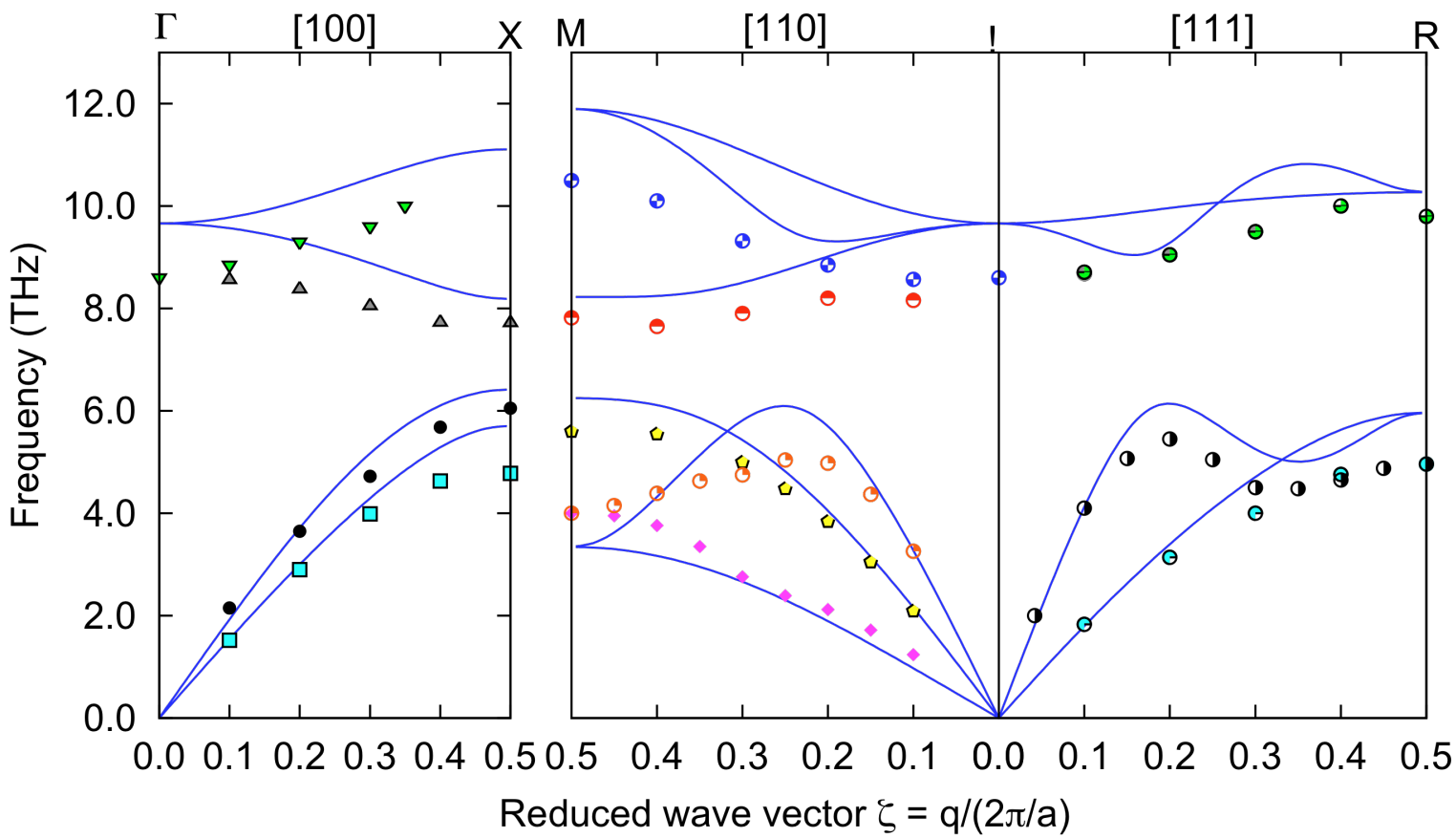

Thermal expansion of B2-NiAl

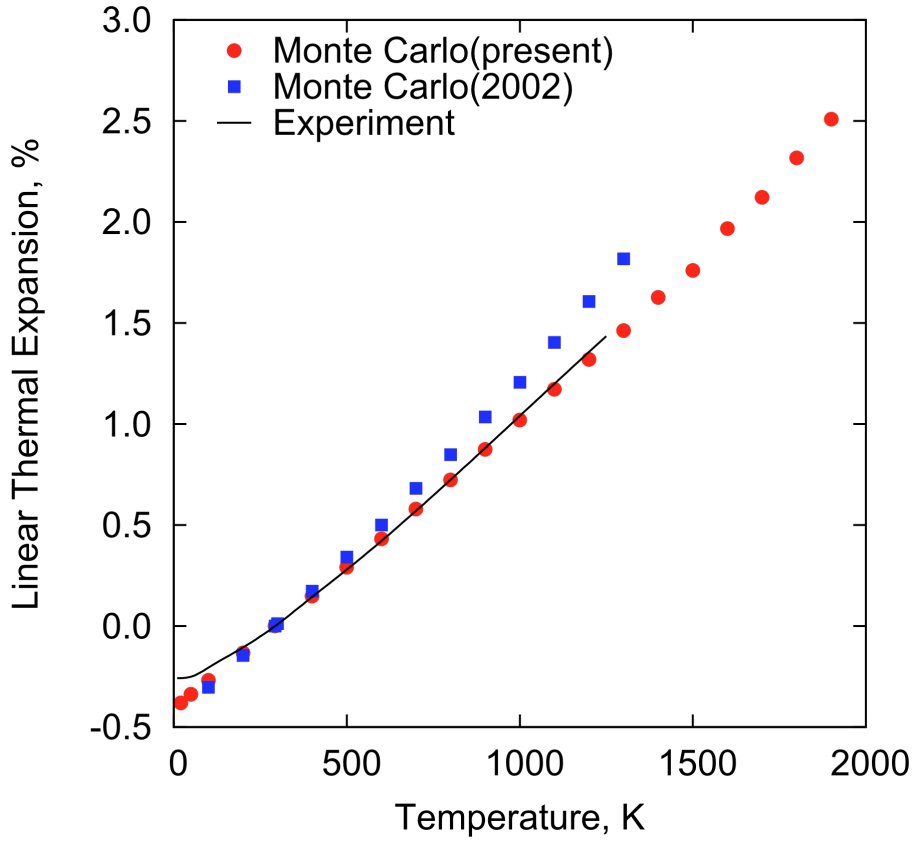

- Monte-Carlo method
- Thermal expansion relative to room temperature
- Significant improvement relative to the “B2-potential” (without fitting)

Properties of Ni_3Al

Lattice properties

	Experiment	EAM (present)	Ni_3A-potential
a_0 (A)	3.57	3.5331	3.571
E_0 (eV)	-4.62	-4.6315	-4.626
c_{11} (GPa)	230	238	236
c_{12} (GPa)	149	166	154
c_{44} (GPa)	132	130	127

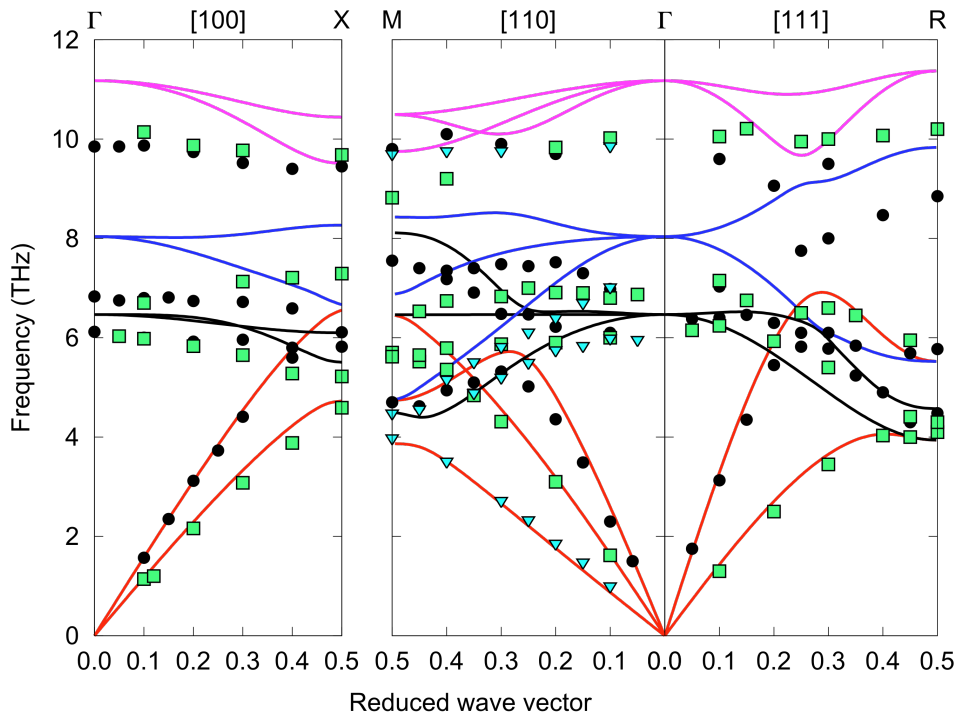

Phonon frequencies (THz)

- Improved phonon frequencies
- Reasonable elastic constants

Deformation paths between structures

Bain path

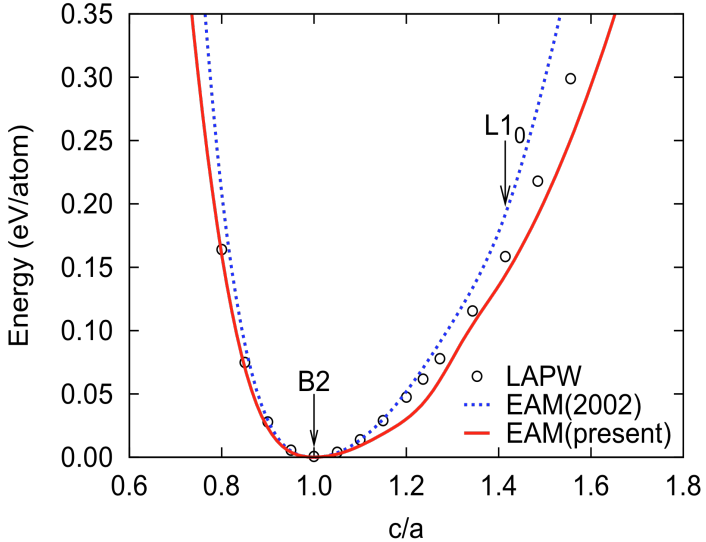

Trigonal path

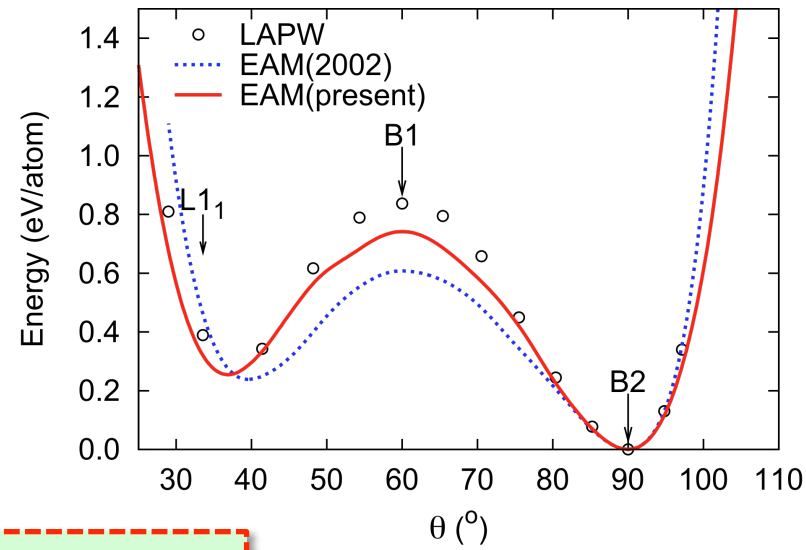

$V=V_{B2}=const$

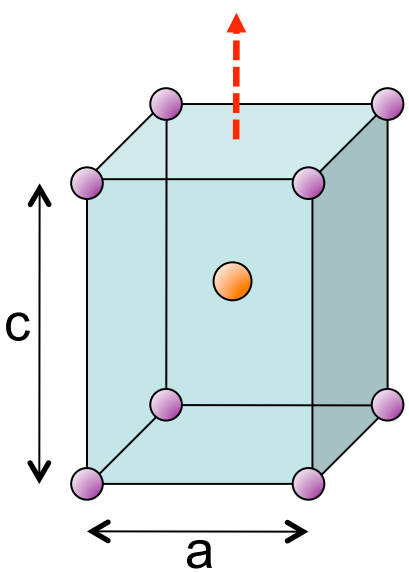

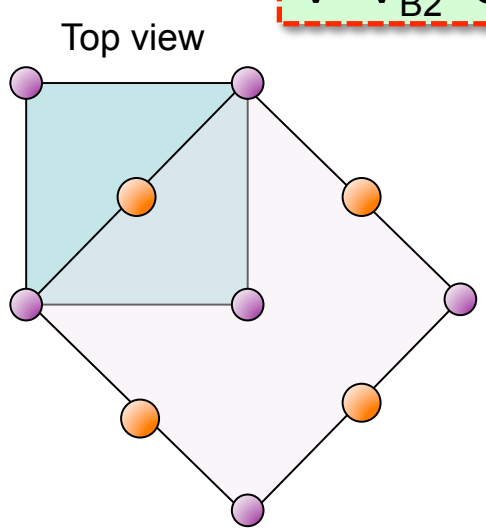

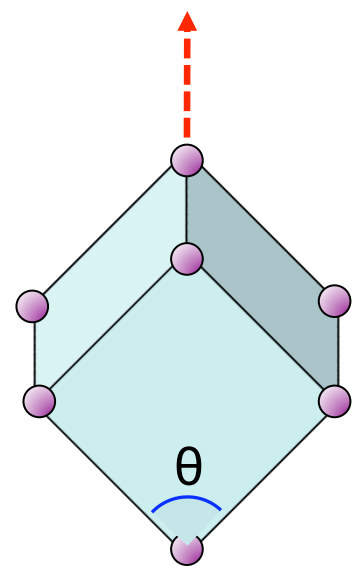

Phase stability in the Ni-Al system

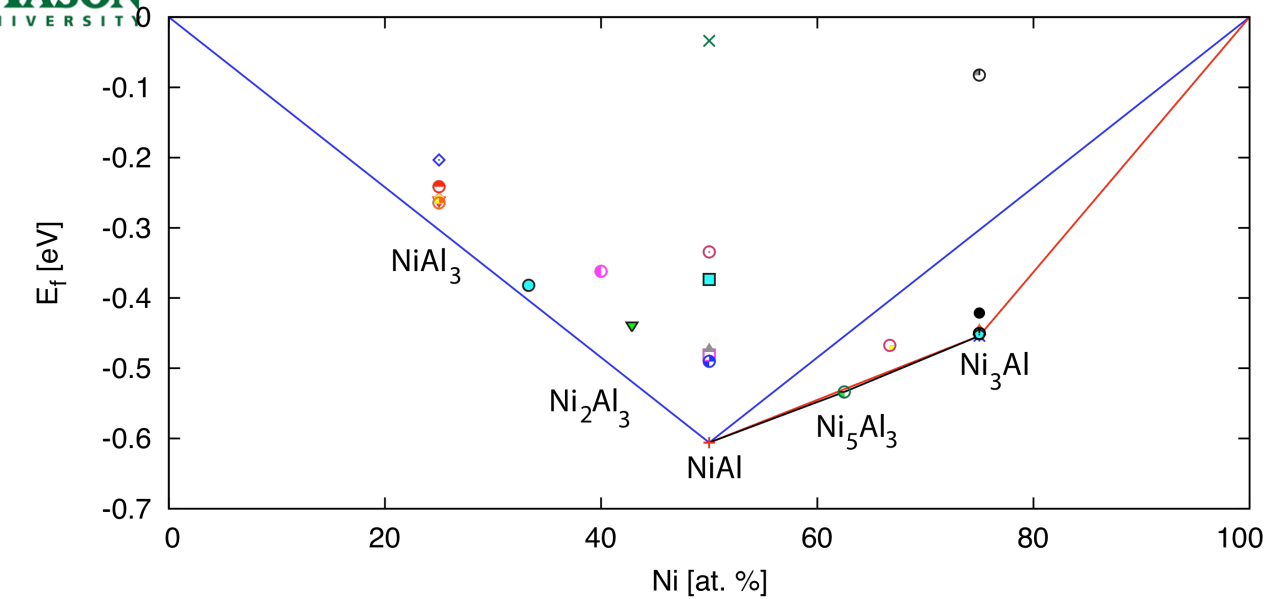

B2:NiAl*
B1:NiAl
L1$_2$:Ni$_3$Al*
L1$_0$:NiAl
B32:NiAl
L1$_1$:NiAl
D0$_{22}$:NiAl$_3$
D0$_{23}$:Ni$_3$Al
D0$_{23}$:NiAl$_3$
D0$_{19}$:Ni$_3$Al
D0$_{19}$:NiAl$_3$
D0$_{11}$:Ni$_3$Al
D0$_3$:Ni$_3$Al
D0$_2$2:Ni$_3$Al
40:NiAl
L1$_2$:NiAl$_3$
Ga$_4$Ni$_3$:Ni$_3$Al$_4$
D0$_3$:NiAl$_3$
D0$_{11}$:NiAl$_3$*
Ga$_3$Pt$_5$:Ni$_5$Al$_3$*
B20:NiAl
D5$_{19}$:Ni$_2$Al$_3$*
C11$_b$:NiAl$_2$
C11$_b$:Ni$_2$Al

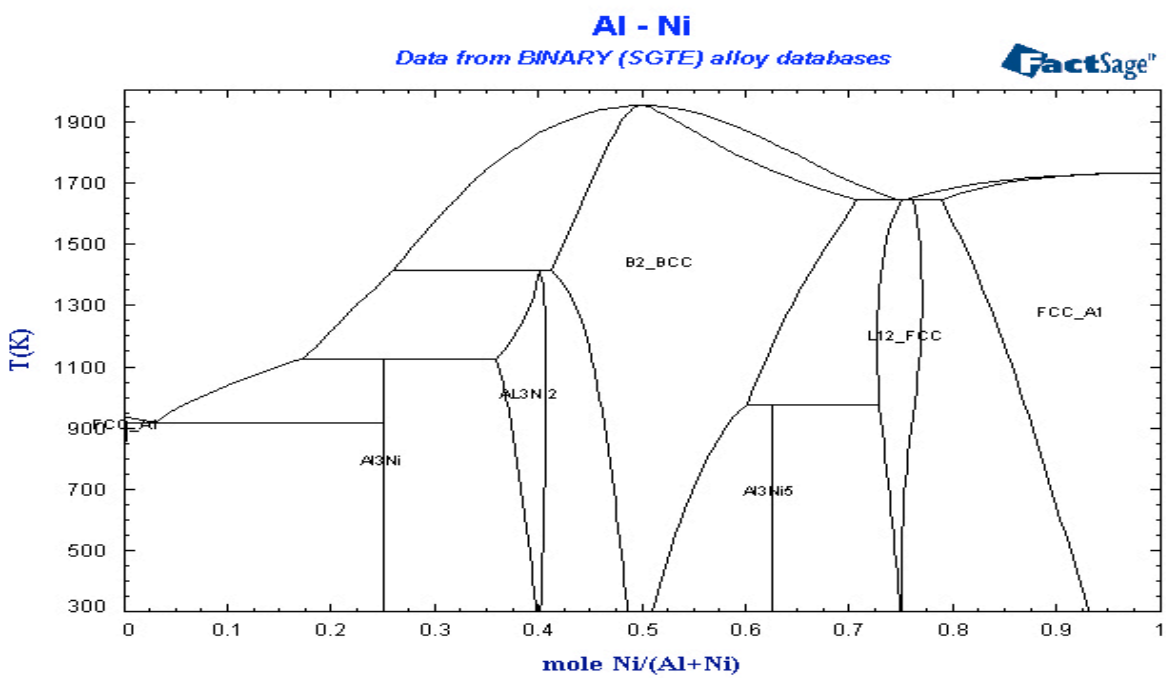

Phase stability is excellent on the Ni-rich side but only fair on the Al-rich side

Summary for the Ni-Al potential

- Reproduces many properties of B2-NiAl and $L1_2$-Ni_3Al in better agreement with experimental and *ab initio* data than previous potentials for the Ni-Al system
- Demonstrates good "transferability" to various configurations and chemical compositions
- Should be suitable for simulations of mechanical properties
- The end-members are the "Ni-04" and "Al-99" potentials

Investigation of the martensitic transformation in Ni-Al shape-memory alloys

NiAl shape memory alloys: background

- **Shape memory effect** in Ni-rich Ni_xAl_{1-x} alloys (x = 0.60-0.64) was discovered in the early 1970s.
- The shape memory effect is explained by a **martensitic phase transformation** B2 ➔ $L1_0$. The transformation does not require any diffusion and occurs at low temperatures.
- The martensitic structure usually contains multiple twins and stacking faults. The stacking faults can form long-period ordered structures such as 7M.
- The transformation is accompanied by a significant hysteresis.
- The martensite-start (M_s) and austenite-finish (A_f) temperatures, as well as the martensite structure depend sensitively on the chemical composition, cooling/heating rate, the microstructure (grain boundaries, dislocations, etc.) and other factors.
- Annealed martensite may contain ordered precipitates of Ni_5Al_3 and/or Ni_3Al.
- Martensitic transformation at the crack tip in B2-NiAl was found experimentally and by simulations.

Where is it on the phase diagram?

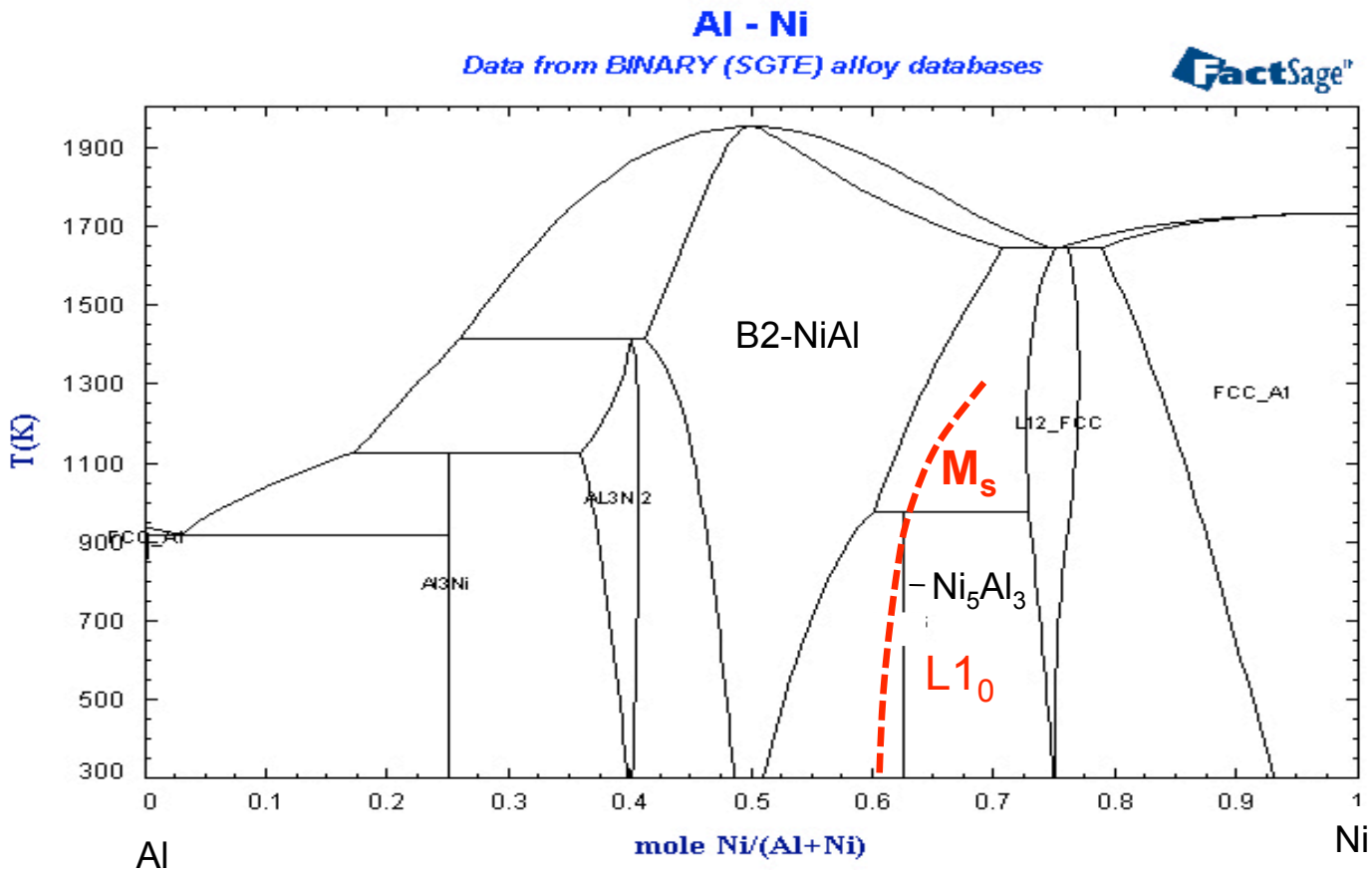

Atomistic simulations of the NiAl martensite:
Status of the field

- Clapp and co-workers (1990s) were the first to study this transformation, focusing on the effect of grain boundaries, surfaces and other defects. Used the Voter-Chen Ni-Al potential (1987), which unfortunately incorrectly predicts $L1_0$ (not B2) to be the ground state for the 50:50 composition.
- Lazarev et al. (2004, 2005) studied the transformation using the potential of Farkas et al. (1995) who refitted the Voter-Chen potential to give the correct ground state. Examined the effects of composition, stresses and defects.
- Guo et al. (2007) simulated crack growth in B2-NiAl and found the martensitic transformation at the crack tip. Used the Farkas potential.
- Many authors (e.g. Ackland, Elliott, Van der Ven) published excellent studies of martensitic transformations in other systems.

Crystallography of the B2-$L1_0$ transformation

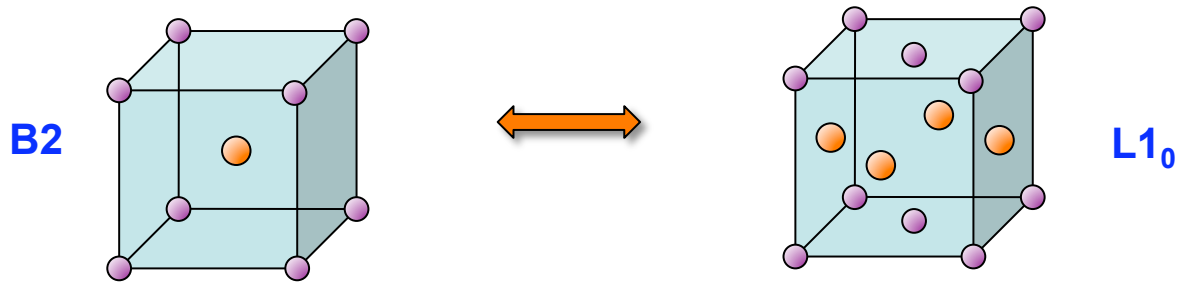

Bain mechanism:

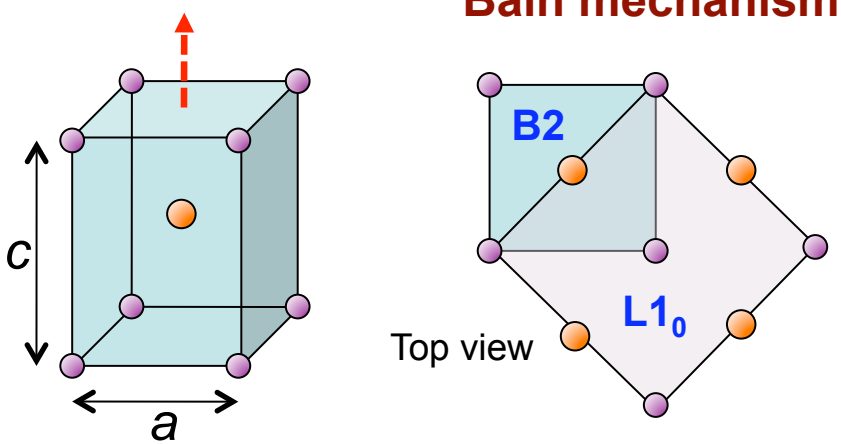

B2: $c/a = 1$ $L1_0$: $1 < c/a < \sqrt{2}$

$\{110\}B2 \rightarrow \{111\}L1_0$

Shuffling mechanism:

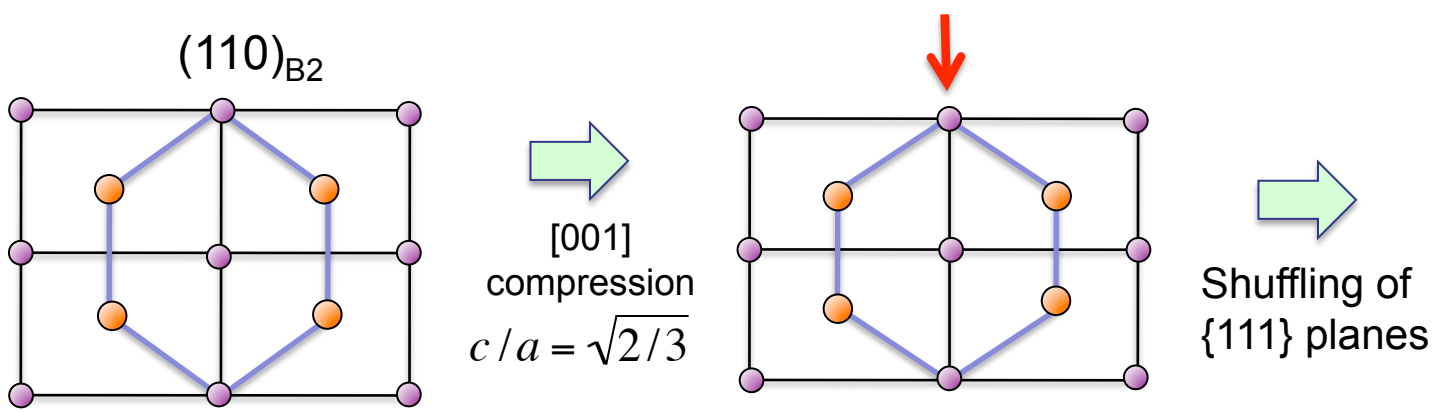

$L1_0$ **twins**

Methodology of simulations

- The new Ni-Al potential.
- Rectangular simulation block with fully periodic boundary conditions. Initial structure B2. Orientations of the axes: [-110], [110], [001].
- Grand-canonical Monte Carlo (NPT) simulations at T = 1200 K with chemical potentials adjusted to give desired Ni-rich chemical compositions.
- Switch to MD simulations in the NPT ensemble at the same temperature and fixed values of the stresses σ_{xx}, σ_{yy} and σ_{zz}.
- Decrease temperature down to 0 K and monitor the block dimensions and energy. Observe the martensitic transformation.
- Increase temperature up to 1200 K and observe the austenitic transformation
- Cooling/heating rate 10^{11} K/s affects the M_s and A_f temperatures.
- Repeat at different tensile/compressive stresses σ_{zz} (with $\sigma_{xx} = \sigma_{yy} = 0$) to study the stress effect on the transformations.
- Repeat in the presence of a (110) APB, open surface, dislocations – to model microstructure effects

B2-$L1_0$ transformation path at T = 0 K

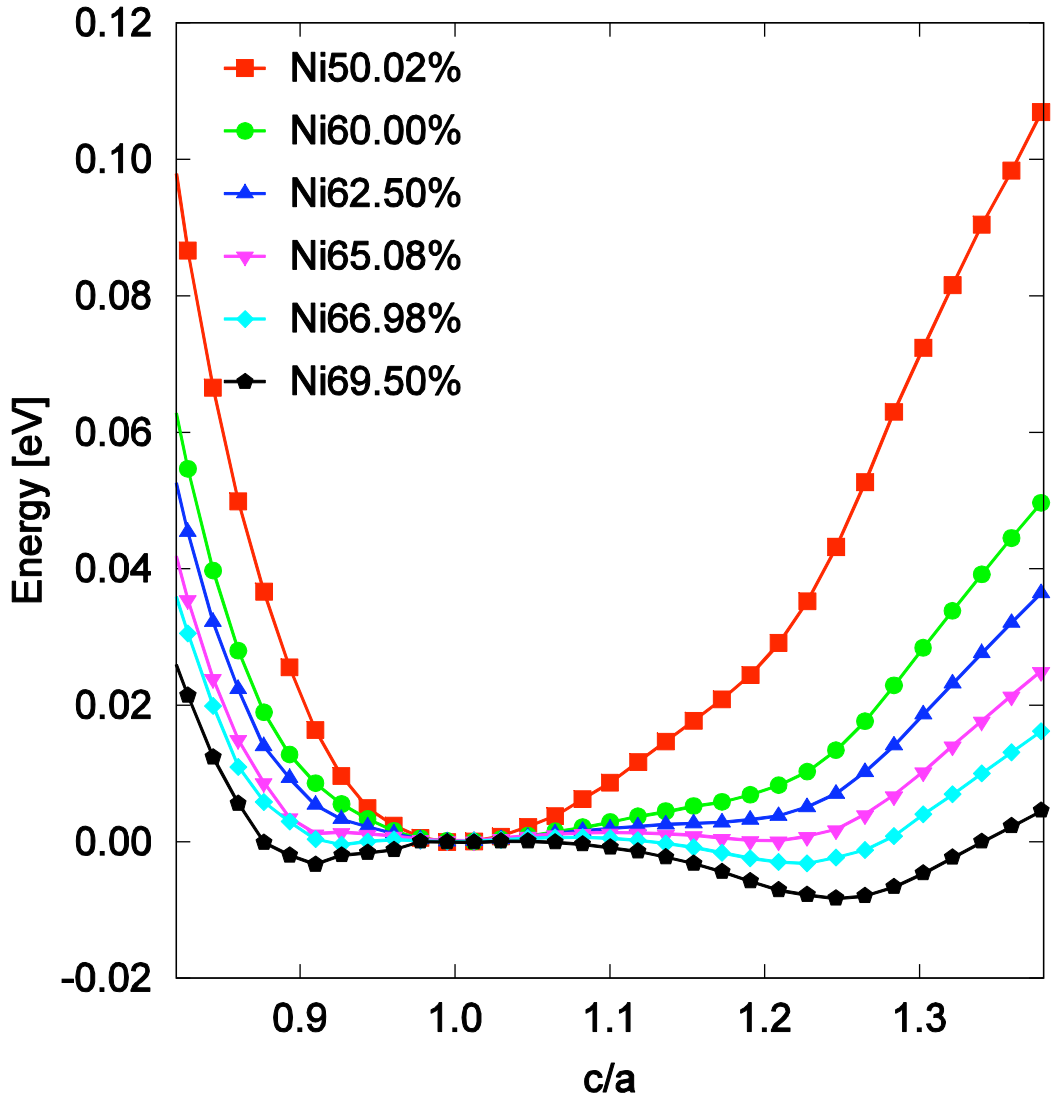

Optimized V

Demonstration of the shape memory effect

Perfect simulation block, σ_{zz} = 280 MPa

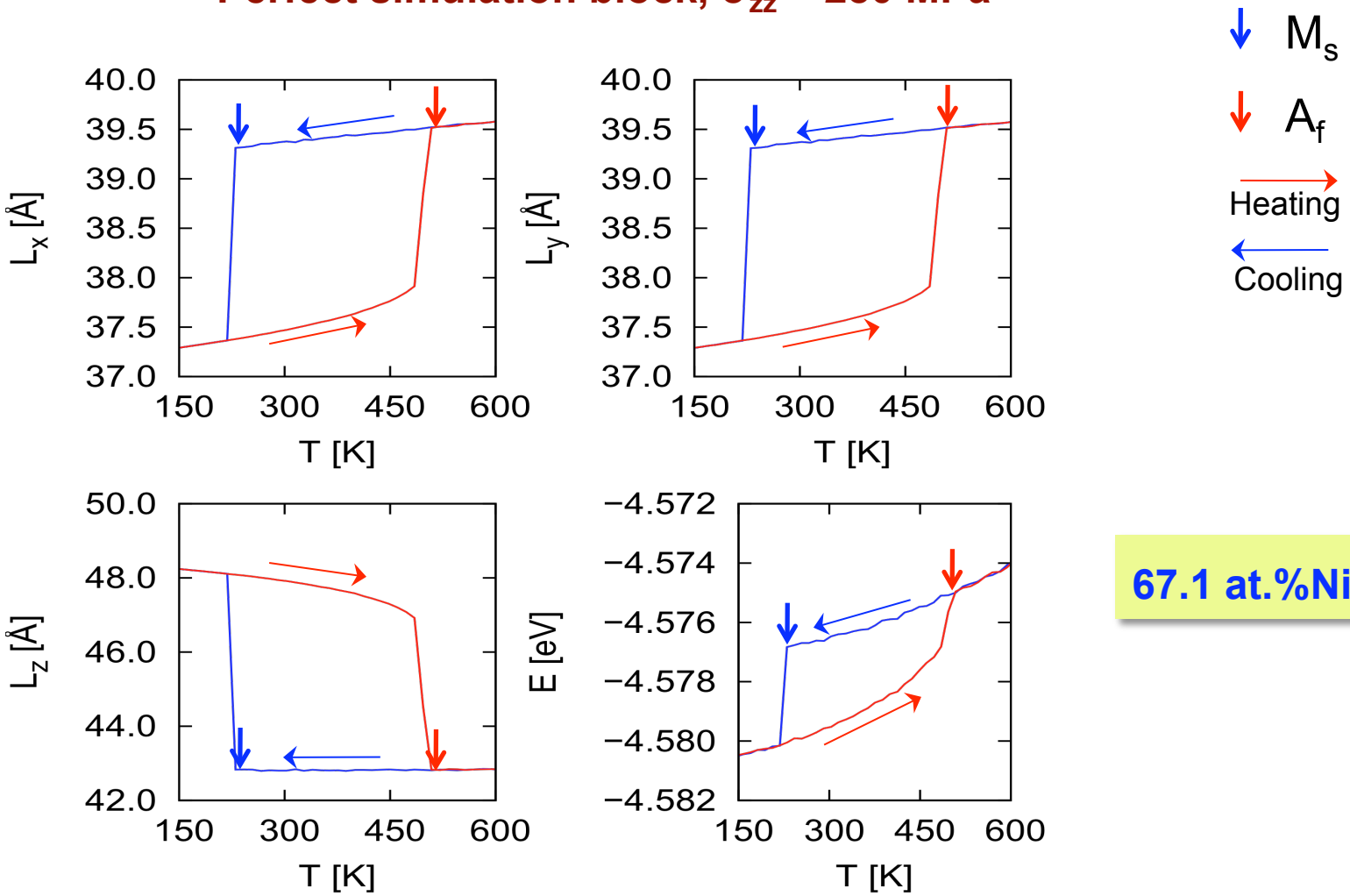

67.1 at.%Ni

Complete reversibility of the crystal structure and shape!

Demonstration of the shape memory effect

Simulation block with a single APB

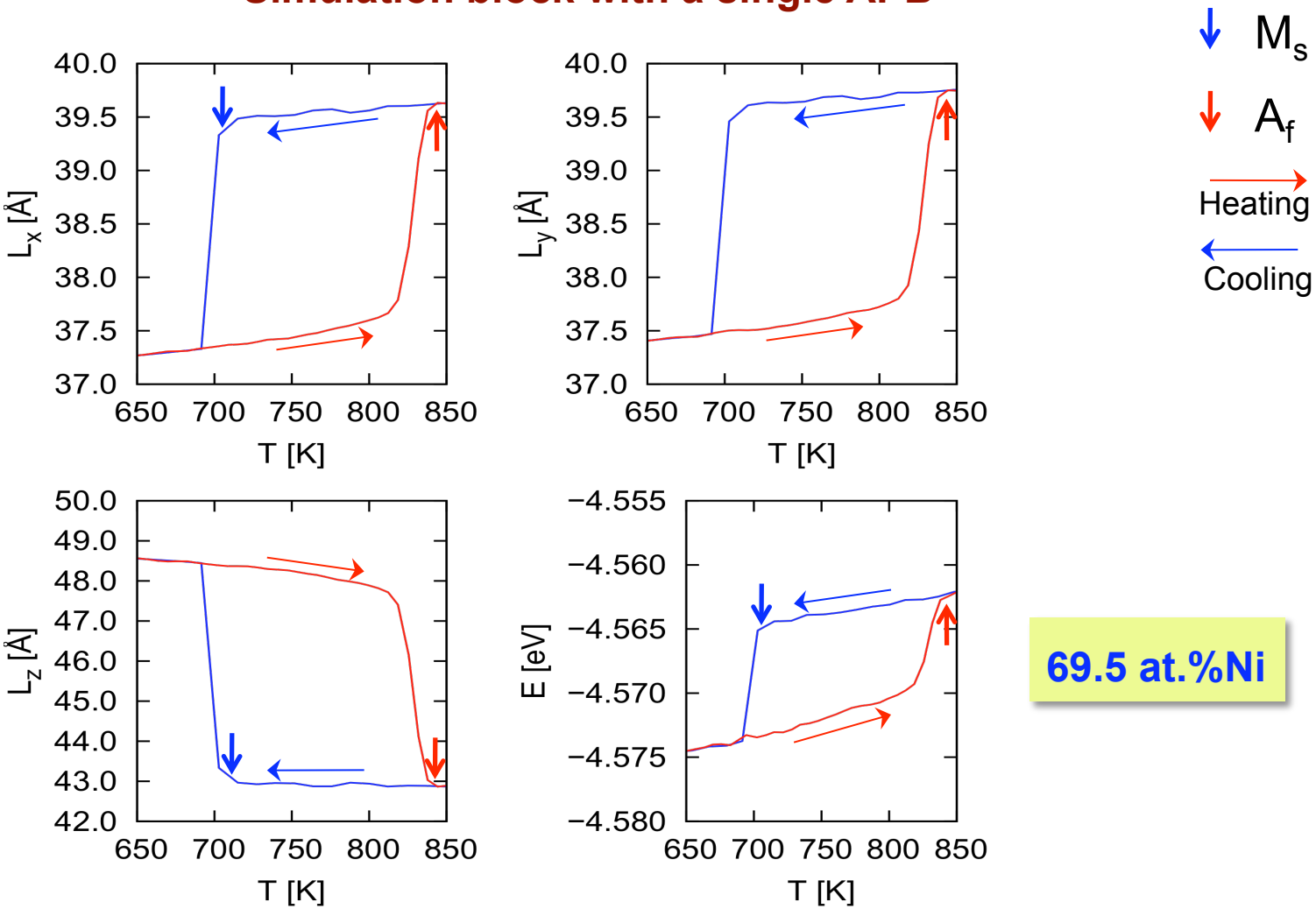

69.5 at.%Ni

Complete reversibility of the crystal structure and shape!

How fast does this happen?

69.5 at.%Ni σ_{zz} = 280 MPa

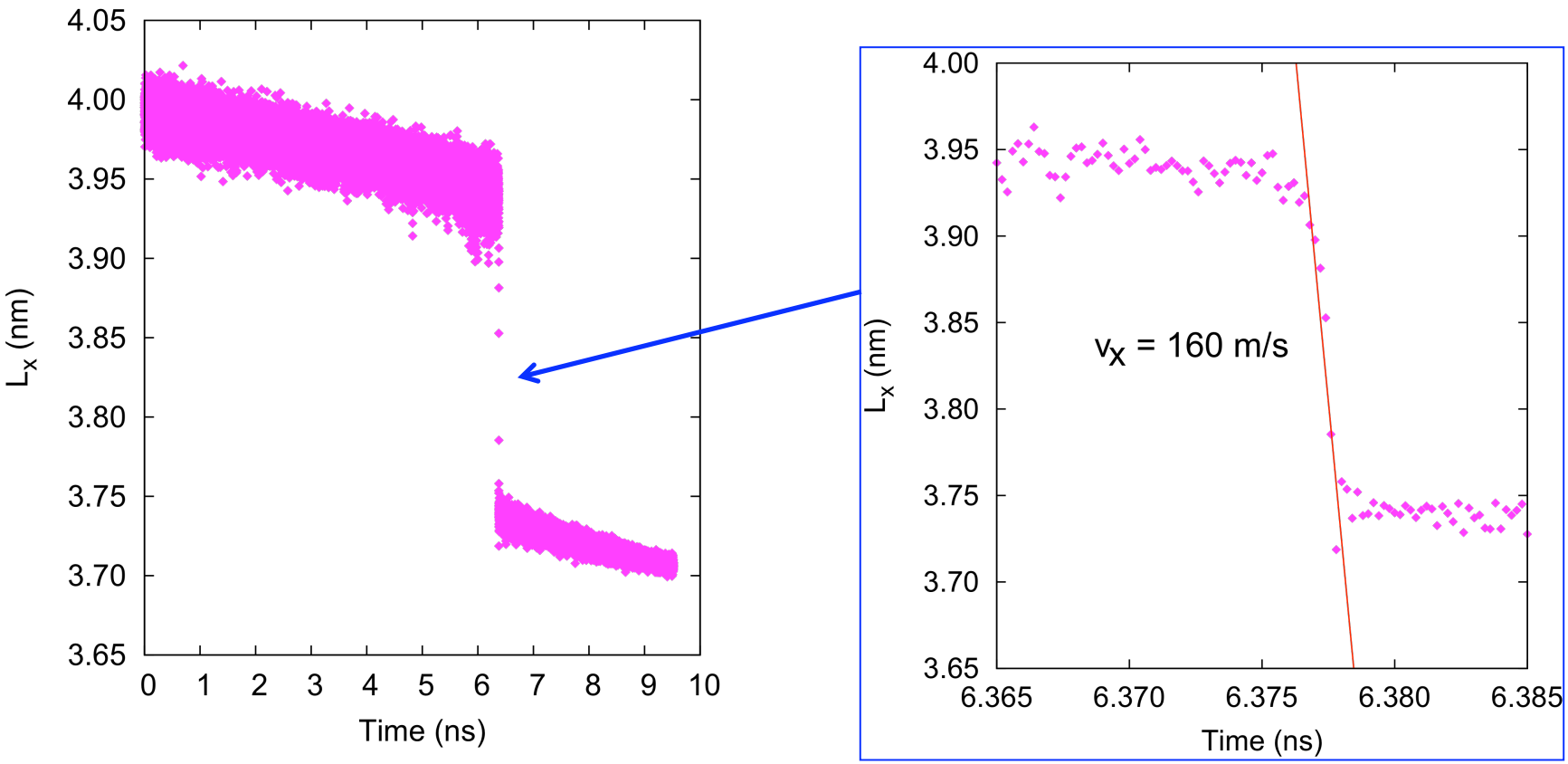

Typical speeds at M_s are 100-300 m/s

Effect of stress on the transformation

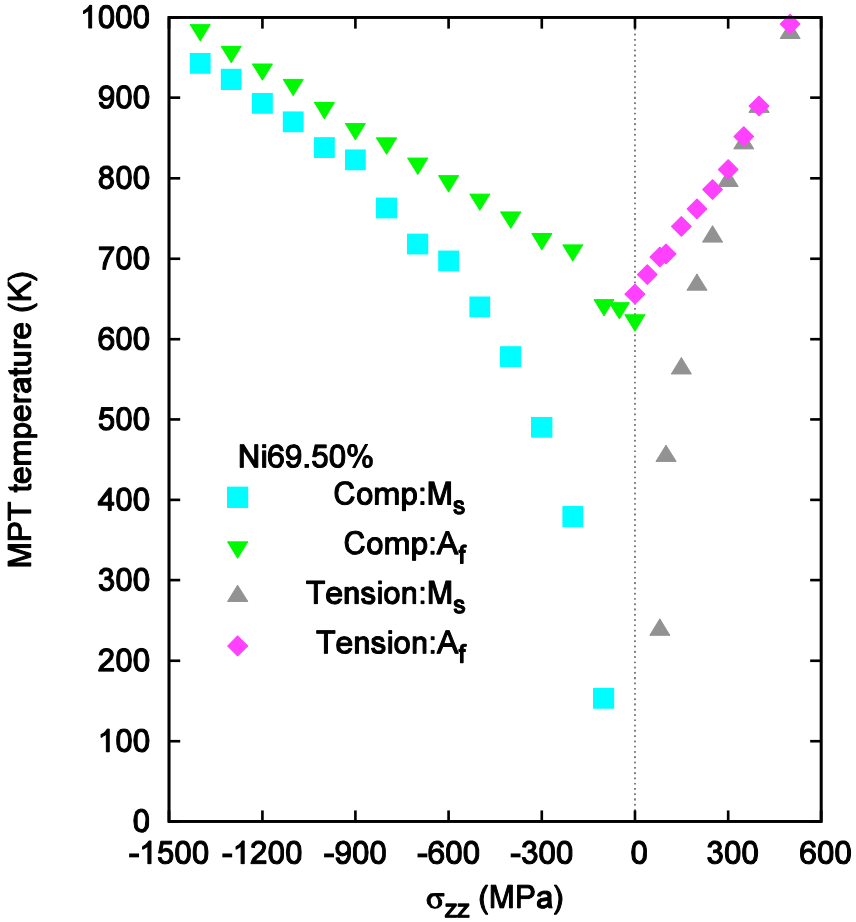

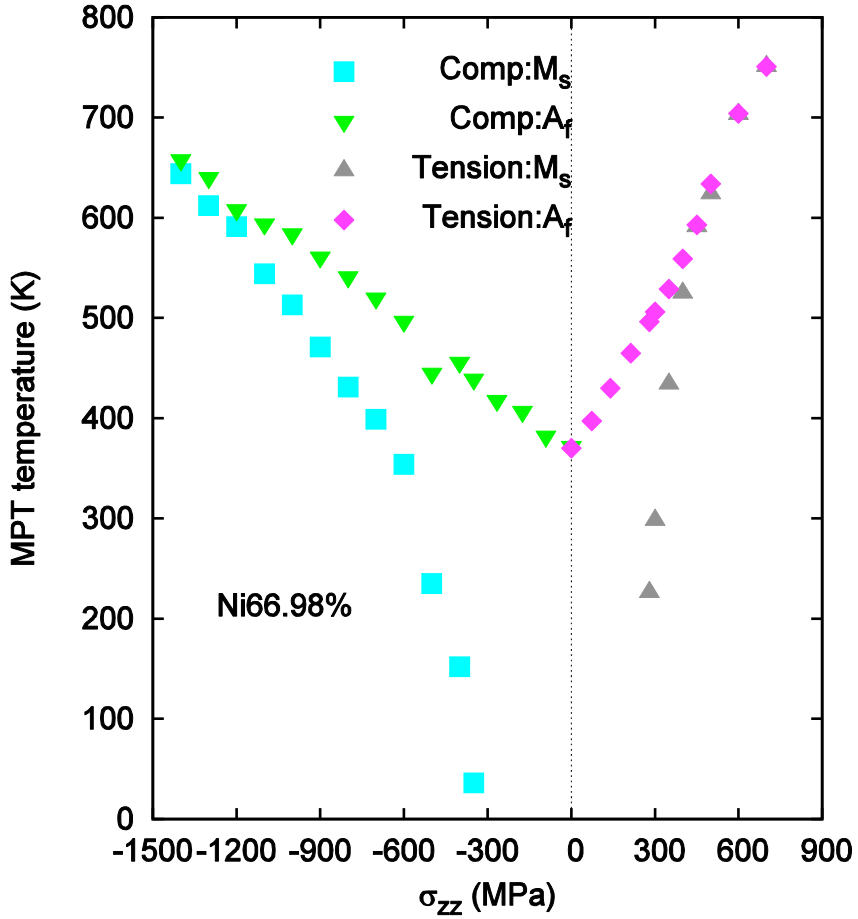

Effect of stress on the transformation

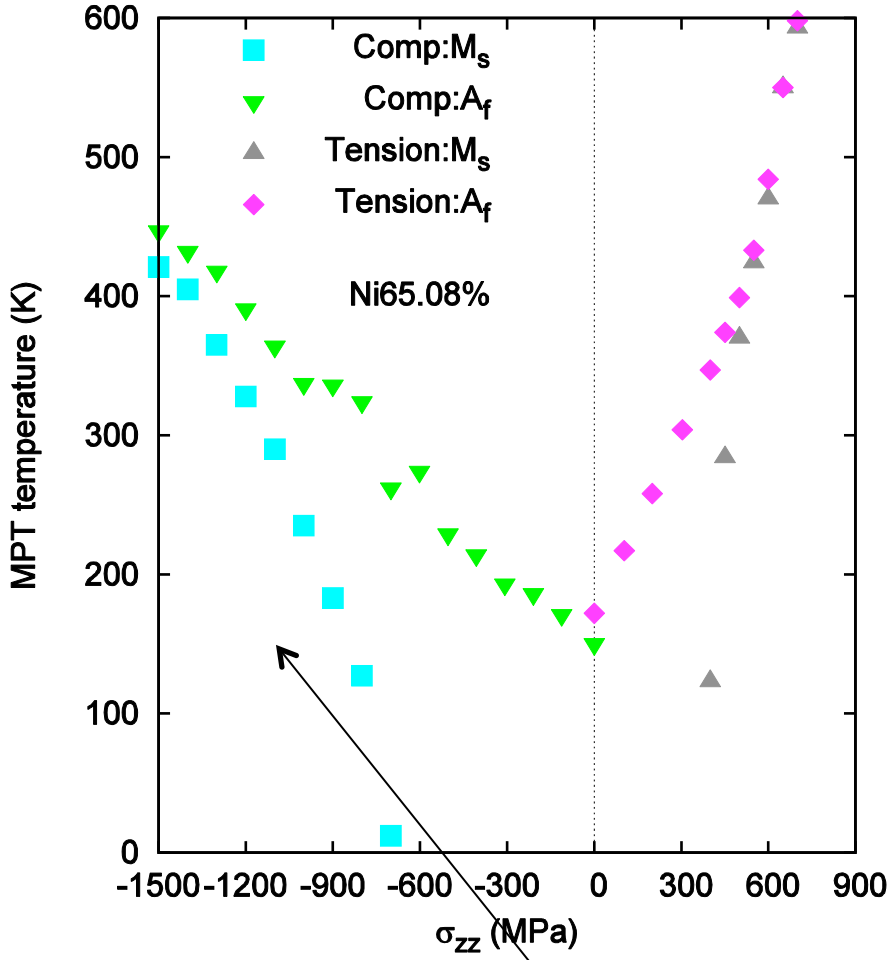

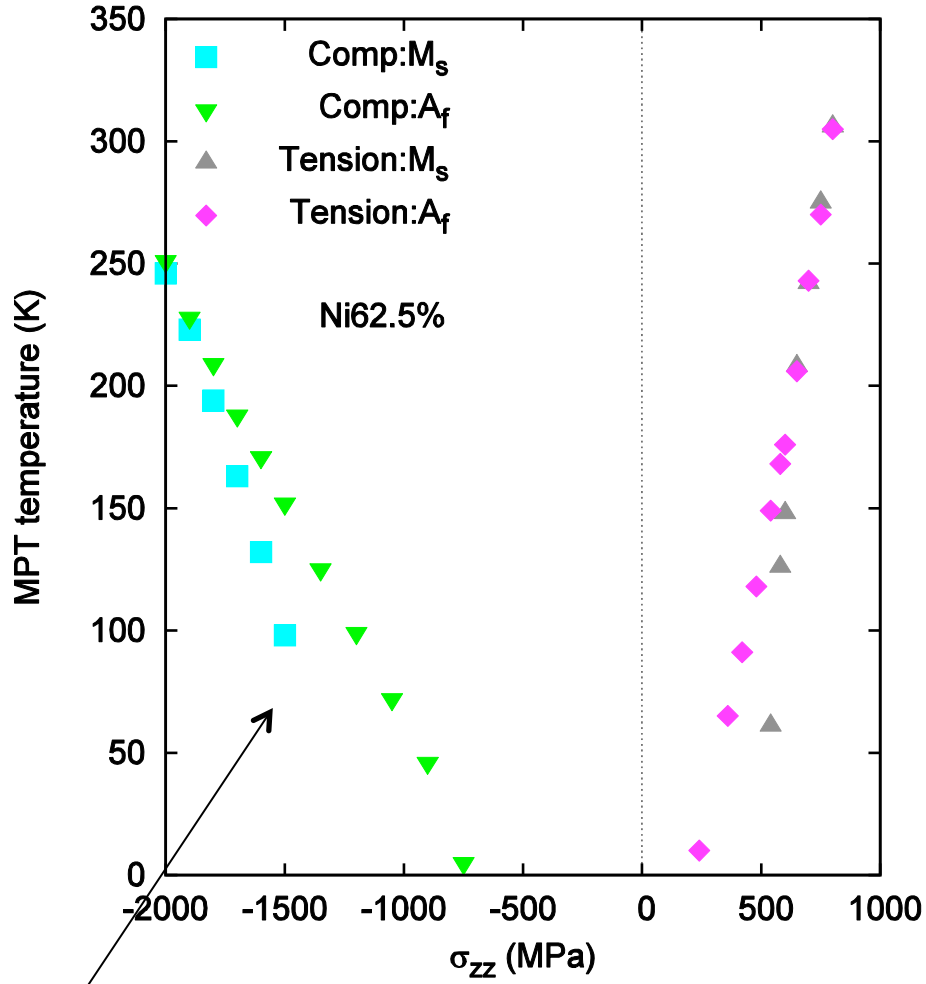

Twinned martensite

Twinned martensite formation

Isothermal annealing at 94 K, compression 800 MPa

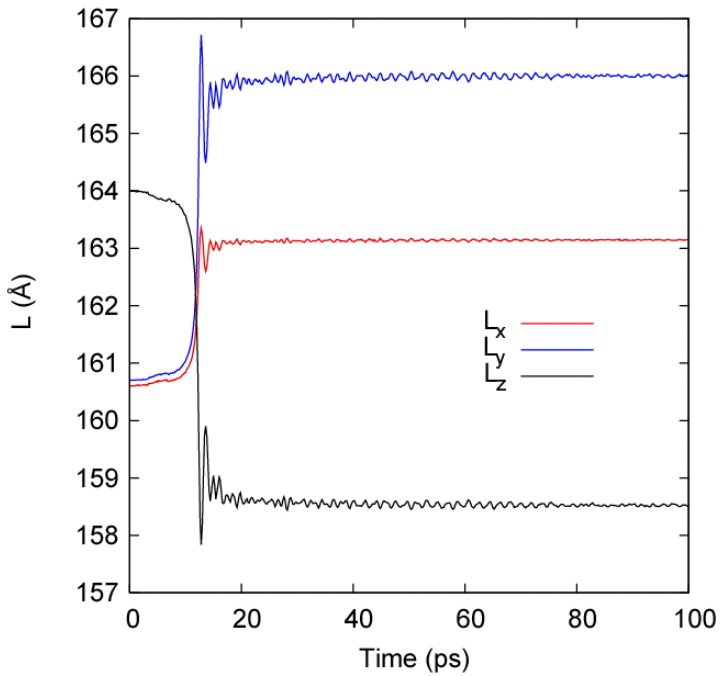

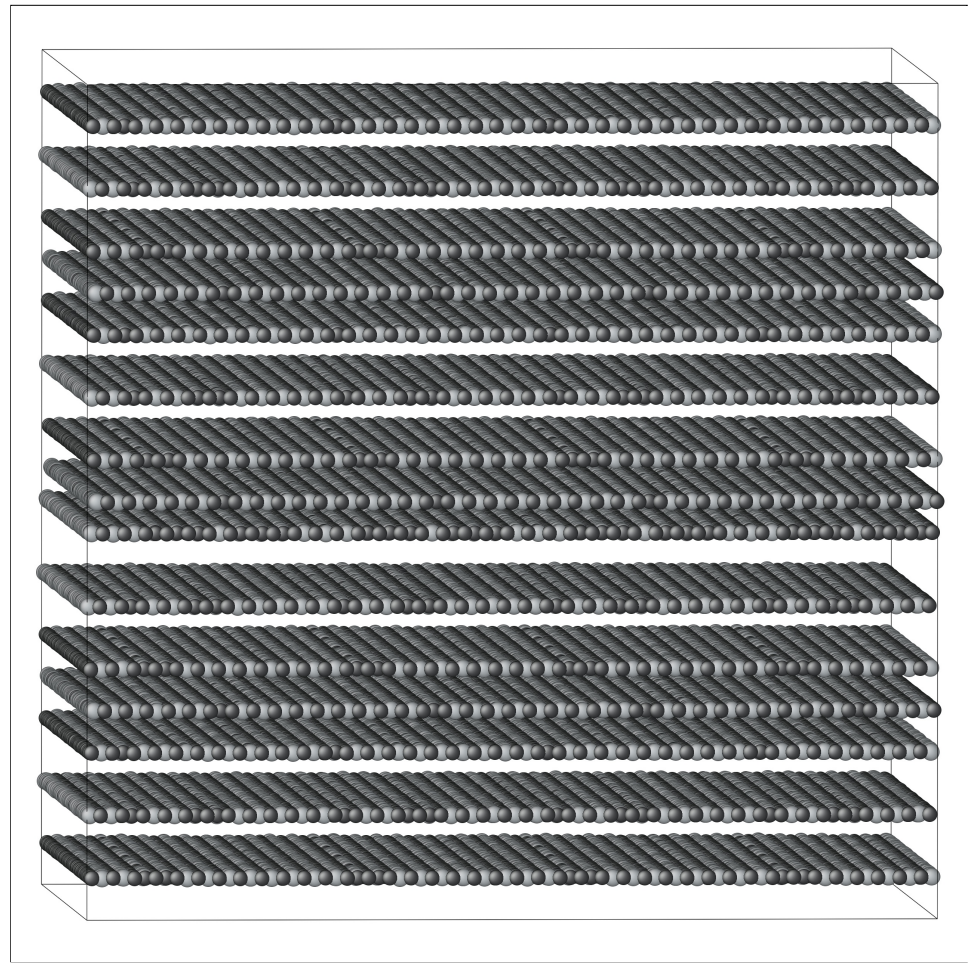

N=384,000 atoms
Composition: 65.08%Ni

Twinned martensite formation

Isothermal annealing at 310 K, compression 200 MPa

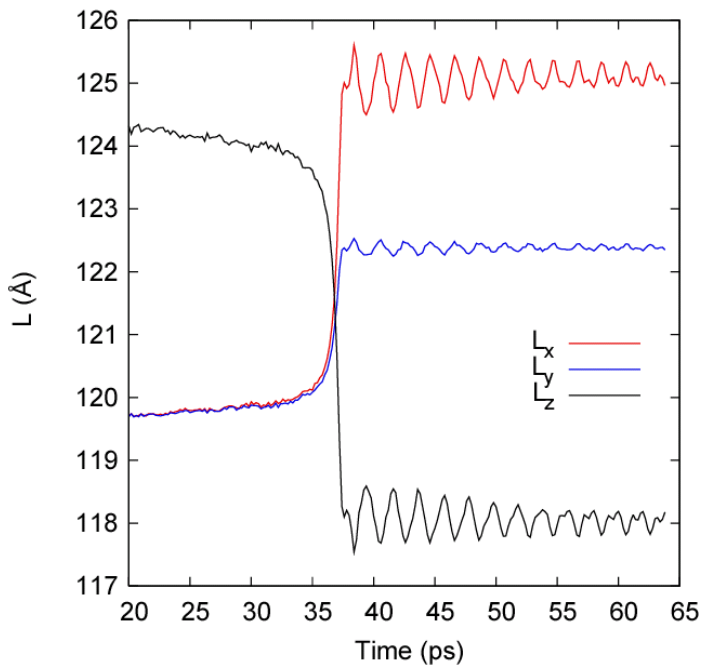

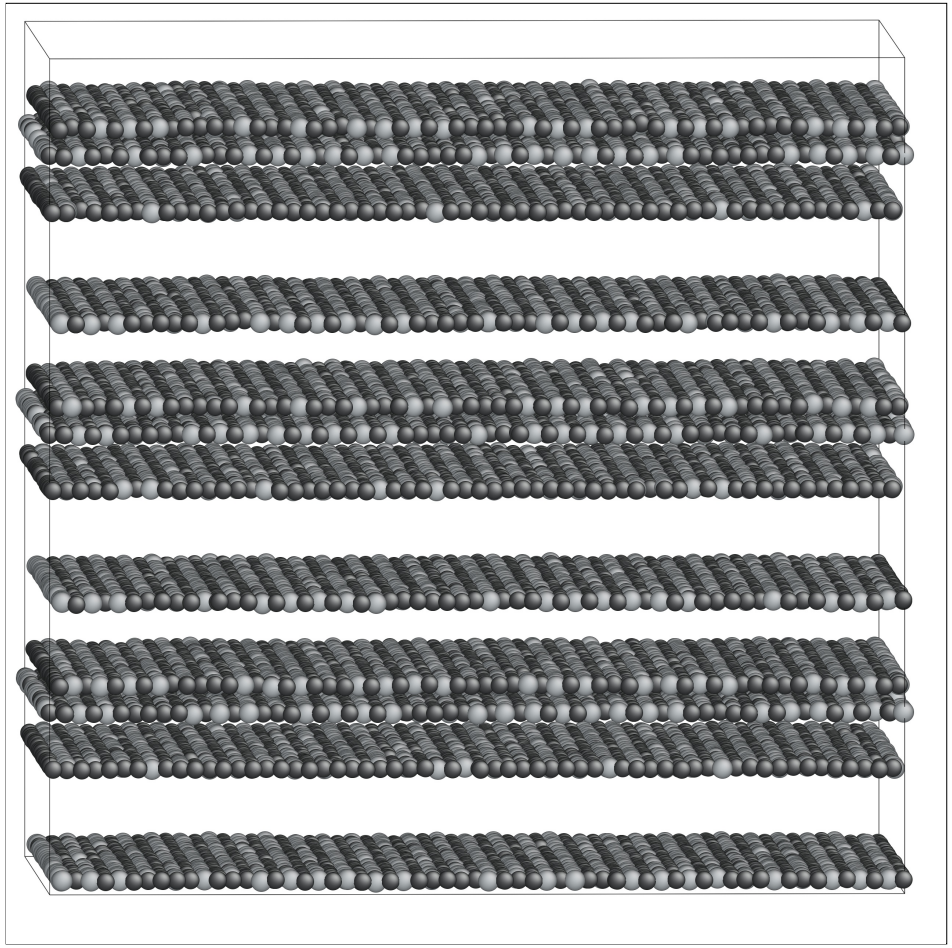

N=162,000 atoms
Composition: 69.50%Ni

Effect of defects on the transformation

69.5at.%Ni

(110) APB: A_f = 827 K; M_s = 700 K
Perfect lattice: A_f = 652 K; M_s = ?

67.0at.%Ni

(110) APB: A_f = 467 K; M_s = 204 K
Perfect lattice: A_f = 372 K; M_s = ?

(110) APB

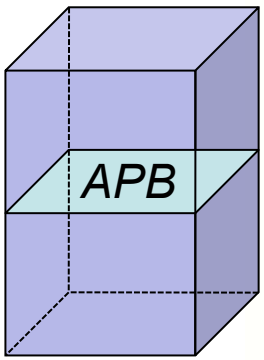

Transformed structure

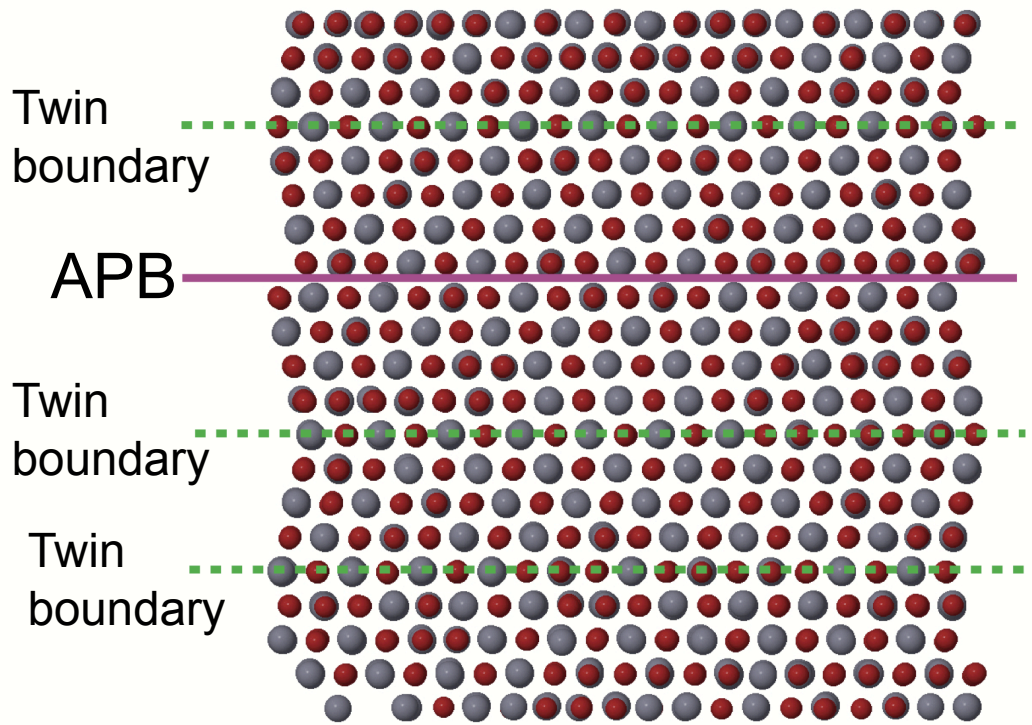

The APB increases M_s and A_f and induces twinning of the martensite

Summary for the martensitic transformation

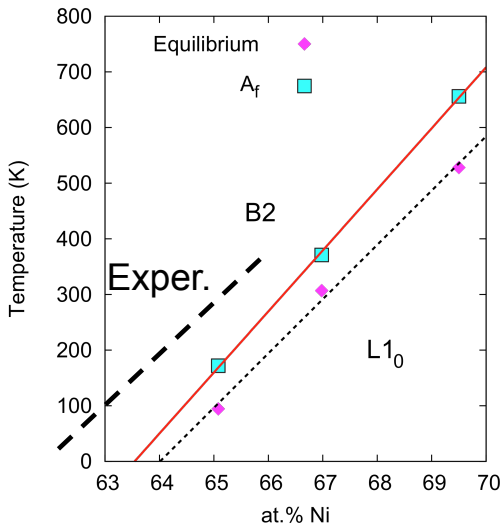

- The transformation is fully reversible both in the perfect lattice and in the presence of defects.
- The transformation is strongly controlled by the nucleation process. The martensite/austenite growth is very fast.
- The transformation temperature depends on the cooling/heating rate. Reducing the cooling rate increases M_s. At the extremely high cooling rates implemented in our simulations, homogeneous nucleation at zero pressure could not be observed.

- Tensile and compressive stresses along [001] increase the transformation temperatures (M_s and A_f) and reduce the hysteresis.
- Lattice defects assist the martensite nucleation and increase M_s. But they can also lead to twinned martensite with relatively high A_f.
- The potential shifts the transformation line to higher Ni concentrations in comparison with experiment. However, experimental samples contain internal stresses and Ni segregation at defects.